ACS OMEGA

Open Access

http://pubs.acs.org/journal/acsodf

Article

Selective Adsorption of Human Testosterone from Plasma Using Zn^{2+}-Loaded Hexanediamine−Chitosan Beads

Huibin Yu,[⊥] Hongqin Ke,[⊥] Tu Chen, Jia Huang, Lei Zhou, and Shenqi Wang*

Cite This: *ACS Omega* 2025, 10, 15393−15399

Read Online

ACCESS | Metrics & More | Article Recommendations

ABSTRACT: This study aimed to develop a novel adsorbent, Zn^{2+}-loaded hexanediamine−chitosan (HDA-CS) beads, for the selective removal of human testosterone from plasma. The preparation involved synthesizing chitosan beads, modifying them with hexanediamine to enhance adsorption capacity and subsequently loading them with zinc ions. The effects of the HDA spacer, Zn^{2+} concentration, and adsorption time on the adsorption percentage for testosterone were systematically investigated through a series of adsorption experiments. Results indicated that the Zn^{2+}-HDA-CS beads achieved a maximum adsorption capacity of approximately 35% within 90 min. The analysis of plasma concentrations of Zn^{2+}, albumin, and sex hormone-binding globulin (SHBG) indicated that the adsorption process involved a complex interaction between testosterone-bound SHBG and albumin for Zn^{2+} binding sites on the beads. Additionally, the adsorbent demonstrated good storage stability and selectivity for testosterone, with minimal impact on total protein content in plasma. These findings highlight the potential of Zn^{2+}-HDA-CS beads as an effective therapeutic option for managing testosterone levels in clinical settings, particularly in patients undergoing androgen deprivation therapy for prostate cancer.

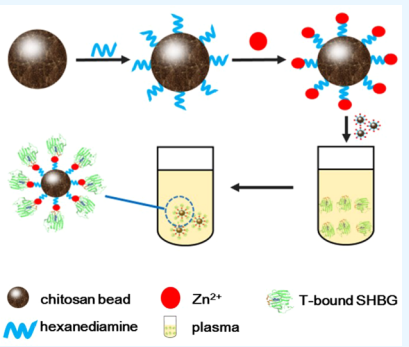

1. INTRODUCTION

Testosterone (T) is the most important plasma androgen in men.[1] It plays a crucial role in the etiology of prostate cancer, as it is essential for the maintenance and growth of the prostate gland.[2] Prostate cancer can regress when androgen stimulation is withdrawn. Currently, androgen deprivation therapy (ADT) is the first-line treatment for prostate cancer.[3] The treatment options for ADT include gonadotropin-releasing hormone (GnRH) agonists and antagonists, as well as bilateral orchiectomy.[4] However, both approaches have significant adverse effects on patients. GnRH agonists and antagonists may increase the risk of cardiovascular disorders and metabolic dysfunction.[5] Orchiectomy is also associated with an elevated risk of Cardiovascular events and has fallen out of favor due to psychological trauma and irreversibility of the procedure.[6]

Both medical therapy and surgical treatment currently fail to yield convincing clinical results. Hemoperfusion presents a promising alternative to ADT. Testosterone is primarily secreted by the testis,[7] and most of it in plasma is protein-bound, and only 1−2% existing in a free form.[8,9] Common hemodialysis cannot effectively remove testosterone from plasma.[10] However, hemoperfusion has been reported to adsorb over 80% of protein-bound toxins.[11] Furthermore, hemoperfusion has been widely utilized in clinical trials, demonstrating positive outcomes for the treatment of intoxication, hepatic failure, renal failure, and sepsis.[12] It is significant to develop a novel adsorbent to remove human testosterone from plasma via hemoperfusion.

Avvakumov et al. reported that the amino-terminal G domain of sex-hormone-binding globulin (SHBG) contains three binding sites for metal ions, with Zn^{2+} binding to site II and III (see Figure 1).[13] Albumin also possesses a major Zn^{2+} binding site.[14] Based on these findings, we designed and prepared Zn^{2+}-loaded cellulose beads coated with chitosan for the removal of human testosterone from plasma.[15]

In this study, we aim to develop an adsorbent with good selectivity for testosterone in human plasma, providing a potential adsorbent for hemoperfusion-based androgen deprivation therapy in prostate cancer. Zn^{2+}, an essential micronutrient for the human body, was selected as a ligand. Chitosan (CS), a widely used material for modified structures and composites,[16,17] was employed to prepare beads with excellent hemocompatibility, serving as the carrier for the adsorbent. Previous research has demonstrated that a specific length of spacer can significantly enhance the adsorption capacity for low-

Received: December 26, 2024
Revised: March 22, 2025
Accepted: April 2, 2025
Published: April 9, 2025

https://doi.org/10.1021/acsomega.4c11595
ACS Omega 2025, 10, 15393−15399

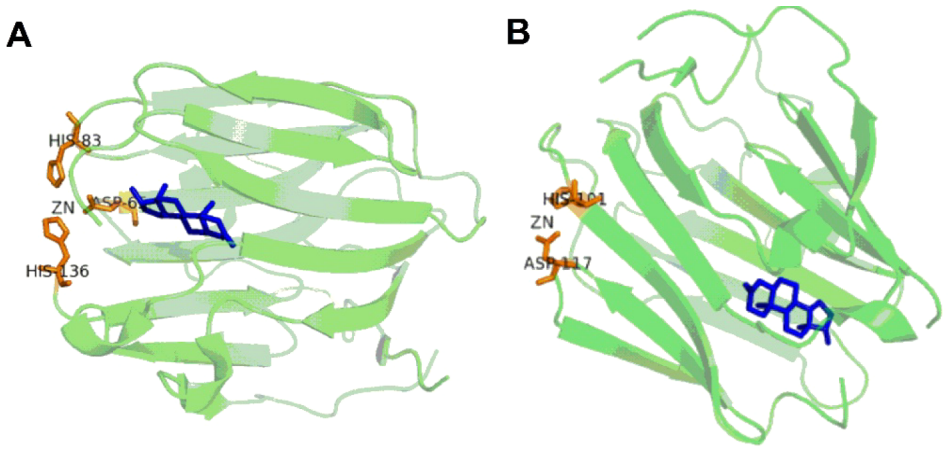

Figure 1. Zinc-binding sites II (Figure 1A) and III (Figure 1B) in the amino-terminal G domain of SHBG. Reprinted with permission from Avvakumov, G. V.; Muller, Y. A.; Hammond, G. L. Steroid-binding specificity of human sex hormone-binding globulin is influenced by occupancy of a zinc-binding site. *J. Biol. Chem* **2000**, 275 (34), 25920−25925. Copyright 2000 Elsevier. PDB code: 1F5F. The active residues in the Zn^{2+} binding site are highlighted in orange, while the steroid within the binding site is depicted in blue.[13]

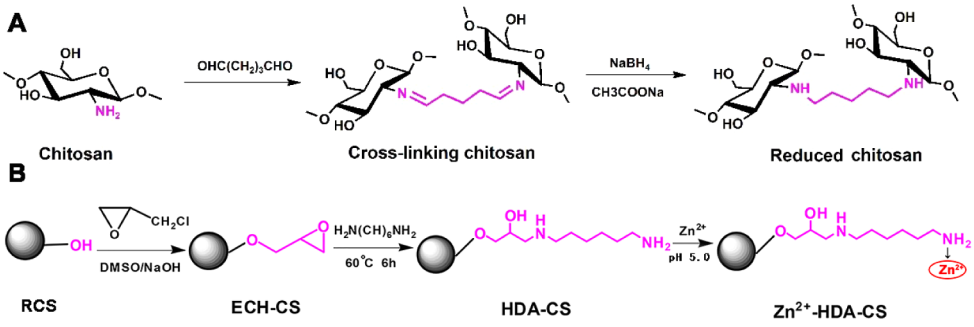

Figure 2. (A) Preparation of reduced chitosan beads; (B) Modification of RCS beads with Zn^{2+}.

density lipoprotein (LDL) and bilirubin.[18,19] Therefore, 1,6-hexanediamine (HDA) was chosen as the spacer to improve the adsorption capacity for testosterone. We prepared Zn^{2+}-loaded chitosan beads as adsorbents for the removal of testosterone from human plasma. Additionally, we investigated the factors affecting the adsorption ability of these adsorbents for testosterone.

2. MATERIALS AND METHODS

2.1. Materials. Chitosan and glutaraldehyde (50% v/v) were obtained from Aladdin Industrial Corporation (Shanghai, China). The deacetylation degree of the chitosan was determined to be 89.4% via acid−base titration, as referenced in the literature.[20] The intrinsic viscosity of chitosan was measured at 495.29 $mL{\cdot}g^{-1}$ at 25 °C using an Ubbelohde viscometer with a capillary diameter of 0.5−0.6 mm. The molecular weight of chitosan was calculated to be 702 kDa using the Mark−Houwink-Sakurada equation. Sodium borohydride, 1,6-hexanediamine, and zinc sulfate heptahydrate were sourced from Sinopharm Chemical Reagent Co. Ltd. (Shanghai, China), while epichlorohydrin (ECH) was obtained from Lingfeng Chemical Reagent Co. Ltd. (Shanghai, China). All other reagents were of analytical grade.

2.2. Plasma Collection. Plasma was collected from several male volunteers aged 18 to 60 years at Shiyan Renmin Hospital, all of whom had routine blood tests that showed no significant abnormalities. The plasma samples were then mixed, aliquoted into EP tubes, and stored at −20 °C until use.

2.3. Preparation of Zn^{2+}-HDA-CS Beads. Reduced chitosan (RCS) beads were prepared using a cross-linking agent in combination with an emulsion technique described by Wang et al. (see Figure 2A).[21] Briefly, a chitosan solution (5% w/v) in aqueous acetic acid solution (5% v/v) was added to a mixture of toluene and Span 80. Glutaraldehyde (40% v/v) was then added into the dispersion medium. The mixture was neutralized with a 5% (w/v) sodium hydroxide solution and heated to 80 °C for 4 h. Chitosan beads, sized between 20 and 40 mesh, were collected and extracted with absolute ethanol in a Soxhlet apparatus for 48 h. Subsequently, they were placed in a flask containing sodium borohydride and sodium acetate and shaken for 12 h. The beads were then collected and washed with deionized water until neutral.

The RCS beads were modified with HDA following established protocols (see Figure 2B).[22,23] Briefly, 1 g of wet beads was mixed in a flask with 6 mL of DMSO, 3 mL of ECH, and 2.25 mL of 2 M NaOH. The resulting suspension was heated to 40 °C and maintained for 4 h, yielding epoxidized RCS (ECH−CS) beads. Subsequently, 1 g of wet ECH−CS beads and 8 mL of 30% (w/v) HDA were added to a ground-glass stoppered Erlenmeyer flask. The mixture was shaken in a thermostatically controlled shaker for 6 h at 60 °C. The liquid was then filtered off, and the beads were washed with deionized water until neutral. The amino groups of chitosan reacted with the aldehyde group of glutaraldehyde, resulting in cross-linked chitosan. Subsequently, the cross-linked chitosan was reduced with sodium borohydride to enhance its stability. The hydroxyl groups of RCS were activated by ECH and coupled with the

https://doi.org/10.1021/acsomega.4c11595
ACS Omega 2025, 10, 15393−15399

amino groups of HDA through an addition reaction involving the epoxy group, resulting in the synthesis of HDA-CS.

Exactly 1 g of wet HDA-CS beads was incubated with 100 mL of an 8 mg·mL^{-1} Zn^{2+} solution at pH 5.0, using zinc sulfate as the source of Zn^{2+}, at 30 °C for 4 h. After washing with deionized water until no Zn^{2+} was detected, Zn^{2+}-HDA-CS beads were obtained.

2.4. Characterization. The epoxy group content on ECH−CS beads was determined using the procedure described by Sundberg.[24] The amino group content on RCS beads and HDA-CS beads was assessed through acid−base titration.[25] Spectrophotometric determinations were performed using a TU-1810 spectrophotometer (Pgeneral, Beijing, China) with zincon for the measurement of Zn^{2+} in the solution.[26] The amount of loaded Zn^{2+} was calculated based on the change in amount before and after incubation, as well as the weight of the beads.

To prevent ice formation from altering the internal structure of beads, HDA-CS beads and Zn^{2+}-HDA-CS beads were frozen at −20 °C to promote the formation of smaller ice crystals. Subsequently, they were transferred to a freeze-dryer (FD-1A-50, Boyikang, China) to remove the water from the beads overnight at −50 °C and 25 Pa vacuum pressure. The freeze-dried beads were then coated with a thin layer of gold powder. The morphologies of the beads were observed using SEM (Sirion 200, FEI, Netherlands).

FTIR-ATR spectra were recorded with a VERTEX 70 spectrometer (Bruker, Germany), scanning from 4000 cm^{-1} to 400 cm^{-1} at room temperature. CS powder, RCS beads, ECH−CS beads, HDA-CS beads, and Zn^{2+}-HDA-CS beads were characterized, respectively.

2.5. Adsorption Experiments for Testosterone. As described in a previous study, 1 g of wet beads was incubated with 3 mL of plasma and stirred for 2 h at 37 °C.[25] The concentration of total testosterone in the plasma was determined using an ELISA KIT (Human T ELISA KIT, MLBIO, China). The adsorption capacity and adsorption percentage were calculated according to the following equations:[19,27]

$$AC = [([C]_B - [C]_A)V_P]/W \quad (1)$$

$$AP = ([C]_B - [C]_A)/[C]_B \times 100\% \quad (2)$$

where AC and AP represent the adsorption capacity and adsorption percentage, respectively; $[C]_B$ denotes the testosterone concentration before adsorption, $[C]_A$ indicates the testosterone concentration after adsorption, V_P is the volume of incubated plasma, and W is the mass of the wet adsorbent.

2.6. Measurement of Zn^{2+}, Albumin, and SHBG Concentrations in Plasma. Exactly 1 g of wet beads was incubated with 3 mL of plasma and stirred for 2 h at 37 °C. Plasma samples were collected at 0, 15, 30, 45, 60, 90, and 120 min intervals. Subsequently, Zn^{2+} concentrations in plasma were determined using a zinc assay kit (Nanjing Jiancheng Bioengineering Institute, China), albumin concentrations were measured using an albumin assay kit (Nanjing Jiancheng Bioengineering Institute, China), and SHBG concentrations were assessed using an ELISA KIT (Human SHBG ELISA KIT, MLBIO, China).

2.7. Measurement of Total Proteins in Plasma. Exactly 1 g of wet beads was incubated with 3 mL plasma and stirred for 90 min at 37 °C. Total protein concentrations were then determined using a total protein quantitative assay kit (Nanjing Jiancheng Bioengineering Institute, China). The adsorption percentage for total proteins was calculated according to eq 2 to evaluate the selectivity of the adsorbent.

2.8. Statistical Analysis. All data were expressed as mean ± SD and analyzed for statistical significance using Student's t test. P-values less than 0.05 were considered statistically significant.

3. RESULTS AND DISCUSSION

3.1. Properties of Zn^{2+}-HDA-CS Beads. An overview of the properties of Zn^{2+}-HDA-CS beads is provided in Table 1.

Table 1. Properties of Zn^{2+}-HDA-CS Beads (n = 3)

Parameter	Value
Diameter (mesh, wet)	20−40
Packing density (g·mL^{-1}, wet)	0.625 ± 0.004
Water content (%, m/m)	56.00 ± 1.52
Amino group content on RCS beads (μmol·g^{-1}, wet)	504.8 ± 2.3
Epoxy group content (μmol·g^{-1}, wet)	312.67 ± 8.08
Amino group content on HDA-CS beads (μmol·g^{-1}, wet)	990.33 ± 5.51
Amount of loaded Zn^{2+} (mg·g^{-1}, wet)	101.67 ± 4.62

The amino group content of RCS beads was measured at 504.8 ± 2.3 μmol·g^{-1}. Following the modification of RCS beads with HDA, the amino group content increased to 990.33 ± 5.51 μmol·g^{-1}. Consequently, the amount of loaded Zn^{2+} reached 101.67 ± 4.62 mg·g^{-1}.

3.2. Effect of Zn^{2+} Concentration on Adsorption Percentage. The effect of Zn^{2+} concentration on the amount of loaded Zn^{2+} ligands is illustrated in Figure 3A. The quantity of loaded Zn^{2+} ligands increased with Zn^{2+} concentration, reaching an equilibrium value in an 8 mg·mL^{-1} Zn^{2+} solution. When HDA-CS beads were incubated in Zn^{2+} solutions of varying concentrations, their adsorption percentages differed. As shown in Figure 3B, the adsorption percentage for testosterone increased with rising Zn^{2+} concentration, peaking at an 8 mg·mL^{-1} Zn^{2+} solution.

Although the results indicated an increase in adsorption percentage with the amount of loaded Zn^{2+} ligands, higher Zn^{2+} concentrations did not contribute further to the quantity of Zn^{2+} ligands. This limitation is attributed to the restricted amino group content on HDA-CS beads.

3.3. Effect of Spacer on Adsorption Percentage. To investigate the effect of the spacer on the adsorption percentage, the adsorbent was synthesized using RCS beads or HDA-CS beads in an 8 mg·mL^{-1} Zn^{2+} solution. The adsorption capacities of Zn^{2+}-CS and Zn^{2+}-HDA-CS were 17.26 ± 1.67% (n = 3) and 35.71 ± 4.50% (n = 3) at 90 min, respectively. The adsorption percentage of Zn^{2+}-HDA-CS beads was significantly higher than that of Zn^{2+}-CS beads (p = 0.003). Two factors may contribute to the overall effectiveness of the spacer for testosterone adsorption. First, the aliphatic hydrocarbon chains (4−10 carbon atoms in length) in the spacers may effectively facilitate adsorption involving small ligands and target proteins.[28] HDA, with 6 carbon atoms, may enhance adsorption involving the Zn^{2+} ligand and T-bound SHBG. Second, the use of HDA as a spacer provides more amino groups, resulting in a higher concentration of Zn^{2+} ligands on Zn^{2+}-HDA-CS beads compared to Zn^{2+}-CS beads. Consequently, the use of HDA as a spacer increased the adsorption percentage of Zn^{2+}-HDA-CS beads for testosterone.

3.4. SEM. Figure 4 presents SEM images of HDA-CS beads and Zn^{2+}-HDA-CS beads. Figure 4A,B indicate that HDA-CS

https://doi.org/10.1021/acsomega.4c11595
ACS Omega 2025, 10, 15393−15399

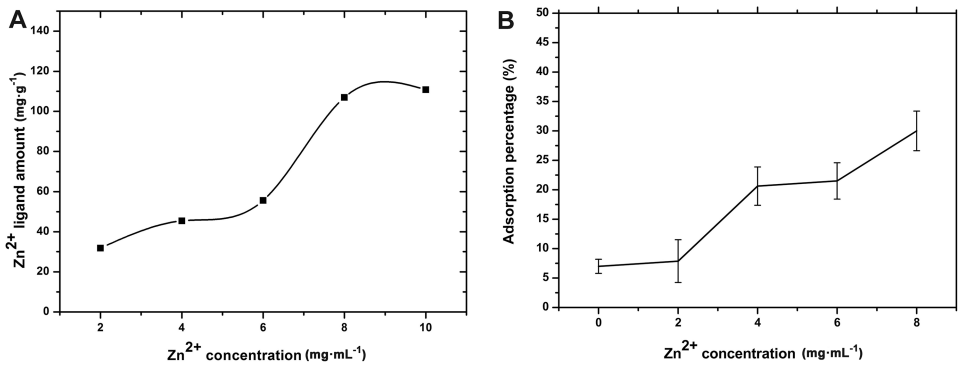

Figure 3. (A) Effect of Zn^{2+} concentration in solution on the amount of loaded Zn^{2+} ligands on Zn^{2+}-HDA-CS beads; (B) Effect of Zn^{2+} concentration in solution on the adsorption percentage for testosterone through Zn^{2+}-HDA-CS beads (n = 3).

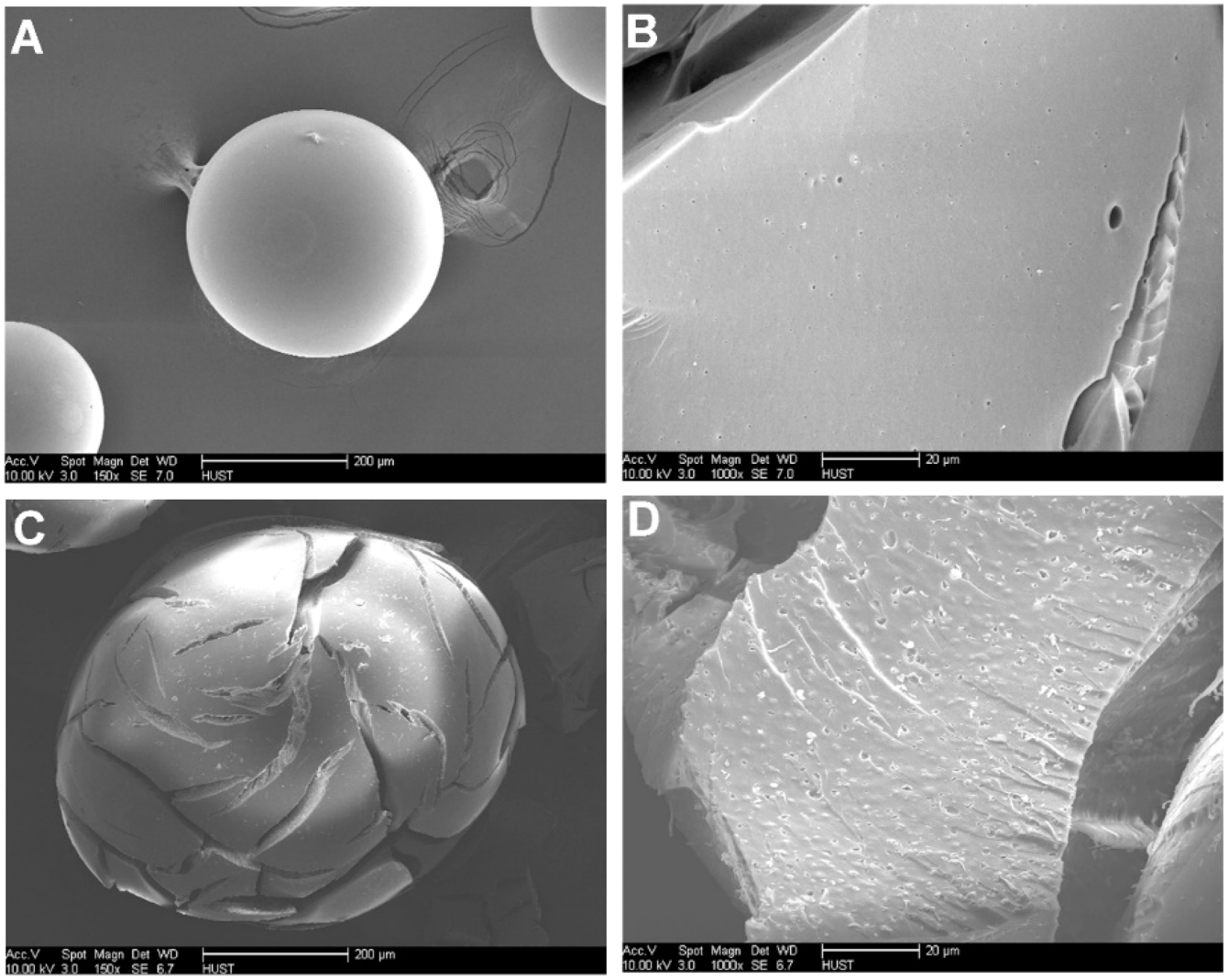

Figure 4. SEM images of (A) the surface of HDA-CS beads, (B) the inner structure of HDA-CS beads, (C) the surface of Zn^{2+}-HDA-CS beads, and (D) the inner structure of Zn^{2+}-HDA-CS beads.

beads are nearly spherical with a smooth surface, although some irregular pores are evident. Figure 4C,D demonstrate that after incubation in a Zn^{2+} solution, the surface morphology of the beads changed. White, crystal-like structures were observed on the surface and within the inner channels of the beads, resembling the SEM images reported by Anitha.[29] This indicates that Zn^{2+} distributed to the internal channels of the adsorbent through its surface pores. The water content of the wet adsorbent was 56%, which also demonstrated that the adsorbent had numerous internal channels connected to the surface. This structure increased the surface area of the adsorbent, enhancing its adsorption rate for testosterone. However, the images also reveal that the pore size of the adsorbent is uneven. Therefore, considering the size of sex hormone-binding globulin, the

https://doi.org/10.1021/acsomega.4c11595
ACS Omega 2025, 10, 15393−15399

preparation process of the adsorbent can be further optimized to produce an adsorbent with appropriate pore size, uniform distribution, and high porosity.

3.5. FTIR-ATR Spectra. The FTIR-ATR spectra of CS powder, RCS beads, ECH−CS beads, HDA-CS beads, and Zn^{2+}-HDA-CS beads are presented in Figure 5. The absorption

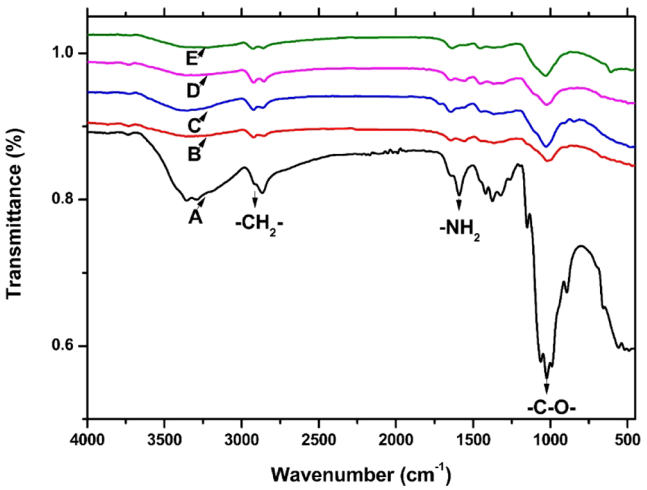

Figure 5. FTIR-ATR spectra of (A) CS powder, (B) RCS beads, (C) ECH−CS beads, (D) HDA-CS beads, and (E) Zn^{2+}- HDA-CS beads.

band from 3400 cm^{-1} to 3300 cm^{-1} is attributed to the stretching vibrations of the N−H and O−H groups. The band around 2960 cm^{-1} to 2840 cm^{-1} is associated with the symmetric and asymmetric stretching vibrations of − CH_3 and − CH_2 groups. The absorption band at approximately 1580 cm^{-1} is assigned to the bending vibration of the N−H group in NH_2. The band from 1170 cm^{-1} to 1030 cm^{-1} corresponds to the combined peaks of the − C−O− group stretching vibrations.[30]

In comparison to the spectrum of CS powder, the band at 2920 cm^{-1} for RCS beads is relatively stronger, while the NH_2 bending band at 1580 cm^{-1} is weakened. These results suggest that glutaraldehyde reacted with the amino groups on chitosan.[30] Compared to the spectra of RCS beads, the band from 1170 cm^{-1} to 1030 cm^{-1} for ECH−CS beads is stronger, indicating that RCS beads reacted with ECH. In the spectrum of HDA-CS beads, the peak at 1580 cm^{-1} is stronger than that of ECH−CS beads, suggesting that HDA reacted with ECH−CS beads, resulting in an abundance of -NH_2 groups. The FTIR spectrum of Zn^{2+}-HDA-CS beads shows a decrease in the intensity of the N−H peak at 1560 cm^{-1}, indicating the formation of a complex band involving N→Zn^{2+}. All these changes demonstrate the successful preparation of Zn^{2+}-HDA-CS beads.

3.6. Effect of Adsorption Time on Adsorption Capacity and Percentage. Figure 6A illustrates the adsorption percentage for testosterone at various adsorption intervals. At 90 min, the adsorbent achieved optimal conditions in plasma, with an adsorption percentage of approximately 35% and an adsorption capacity of 0.0128 nmol·g^{-1} for testosterone.

3.7. Effect of Albumin, SHBG, and Leaked Zn^{2+} on Adsorption Percentage for Testosterone. Although the adsorption percentage for testosterone generally increased, it exhibited fluctuations over time. Consequently, the concentrations of Zn^{2+}, albumin and SHBG in plasma were simultaneously measured during the adsorption of testosterone. The results are presented in Figure 6B. From 15 to 120 min, the changes in adsorption percentage for testosterone and the content of SHBG appeared to be inversely related, while the changes in adsorption percentage for testosterone and the content of albumin showed a similar trend. The concentration of Zn^{2+} also varied over time. Based on these observations, the following adsorption process can be inferred: Initially, albumin was absorbed by Zn^{2+}-HDA-CS beads, reaching an equilibrium value at 15 min. Subsequently, some albumins bound to Zn^{2+} on Zn^{2+}-HDA-CS beads were replaced by testosterone-bound SHBG.

However, from 30 to 45 min, the leakage of Zn^{2+} increased, leading to a decrease in the adsorption percentage for testosterone. From 45 to 90 min, the leakage of Zn^{2+} slowed, and the adsorption percentage for testosterone reached its peak at 90 min. Ultimately, the adsorption percentage for testosterone began to decline as Zn^{2+} leakage increased.

The adsorption of testosterone in plasma is a complex process. During this process, SHBG and albumin in plasma interacted

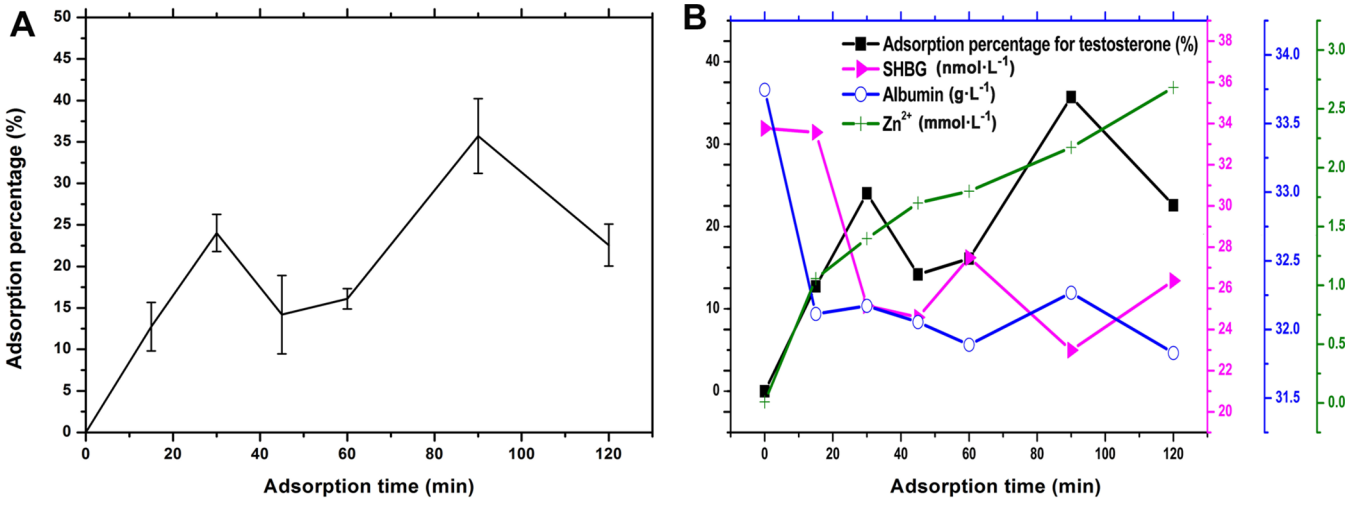

Figure 6. (A)Effect of adsorption time on the adsorption percentage for testosterone (n = 3); (B) Effect of leaked Zn^{2+}, albumin, and SHBG on adsorption percentage for testosterone through Zn^{2+}-HDA-CS beads (n = 3). SHBG, Albumin and Zn^{2+} in Figure 6B represent the concentrations of SHBG, albumin and Zn^{2+} in plasma during the adsorption of testosterone.

https://doi.org/10.1021/acsomega.4c11595
ACS Omega 2025, 10, 15393−15399

with Zn^{2+} on the adsorbent. Specifically, the Zn^{2+} on the adsorbent form coordinate bonds with the Zn^{2+}-binding sites located in the amino-terminal G domain of SHBG (Figure 1). This interaction facilitates the adsorption of testosterone-bound SHBG complexes from plasma, thereby achieving selective removal of testosterone. Although the ratio of leaked Zn^{2+} to the total loaded Zn^{2+} on Zn^{2+}-HDA-CS beads was below 0.5% at 90 min, the leakage of Zn^{2+} still affected the adsorption of testosterone. Formulating the adsorbent into a composite metal−organic framework could potentially enhance the stability of Zn^{2+} on the adsorbent and reduce Zn^{2+} leakage.[31]

3.8. Effect of the Adsorbent on Total Protein Content in Plasma. The total protein concentrations in plasma before and after adsorption were $68.48 \pm 3.04\ g{\cdot}L^{-1}$ and $65.69 \pm 2.31\ g{\cdot}L^{-1}$ ($n = 3$, adsorption time is 90 min), respectively. The adsorption percentage for total proteins was 2.79%. The change in adsorption percentage was less than 5% before and after the adsorption of testosterone, suggesting that Zn^{2+}-HDA-CS beads exhibited good adsorption selectivity.[27]

3.9. Storage Stability. Wet-state Zn^{2+}-HDA-CS beads were sealed and stored at 4 °C in a refrigerator. The initial adsorption percentage of the adsorbent was $28.17 \pm 2.63\%$ ($n = 3$). After 1 month, the adsorption percentage was $27.82 \pm 3.23\%$ ($n = 3$). Compared to the initial adsorption percentage, no significant decrease was observed ($p = 0.921$). This demonstrates that Zn^{2+}-HDA-CS beads are stable and retain their adsorption percentage for testosterone after 1 month of storage. It was crucial to maintain the Zn^{2+}-HDA-CS beads in wet state. When stored in water, Zn^{2+} not only leaks from the Zn^{2+}-HDA-CS beads but also causes the beads to swell. In contrast, when Zn^{2+}-HDA-CS beads are in a dry state, Zn^{2+} crystallizes, blocking the channels of the beads [Figure 4C,D].

4. CONCLUSIONS

In this study, we prepared Zn^{2+}-HDA-CS beads as an adsorbent for the removal of human testosterone in plasma. The adsorbent demonstrated a significant adsorption capacity for testosterone, with the highest adsorption percentage observed at 90 min, approximately 35%. The adsorption of testosterone is attributed to the competition between T-bound SHBG and albumin for Zn^{2+} binding sites on the beads. Additionally, the adsorbent exhibited excellent storage stability and selectivity, making it a potential candidate for the adsorption of human testosterone in plasma.

AUTHOR INFORMATION

Corresponding Author

Shenqi Wang − *School of Life Science and Technology, Huazhong University of Science and Technology, Wuhan 430074, China;* orcid.org/0000-0001-9617-1477; Email: shenqiwang131@hust.edu.cn

Authors

Huibin Yu − *Department of Pharmacy, Renmin Hospital, Hubei University of Medicine, Shiyan 442000, China; School of Life Science and Technology, Huazhong University of Science and Technology, Wuhan 430074, China*

Hongqin Ke − *Department of Pharmacy, Taihe Hospital, Hubei University of Medicine, Shiyan 442000, China*

Tu Chen − *Department of Clinical Laboratory, Renmin Hospital, Hubei University of Medicine, Shiyan 442000, China*

Jia Huang − *School of Life Science and Technology, Huazhong University of Science and Technology, Wuhan 430074, China*

Lei Zhou − *School of Life Science and Technology, Huazhong University of Science and Technology, Wuhan 430074, China;* orcid.org/0000-0003-4125-8502

Complete contact information is available at: https://pubs.acs.org/10.1021/acsomega.4c11595

Author Contributions

⊥H.Y. and H.K. contributed equally to this work. S.W., H.Y., and H.K. conceived and designed the experiments; H.Y. and J.H. performed the experiments; H.Y. analyzed the data; H.K. and T. C. had significant contribution in collection for plasma; H.Y. wrote the paper; S. W. and L.Z. revised the article.

Funding

This research was supported by the National Key Research and Development Program of China (2017YFC1104402), the Initial Research fund from China Scholarship Council and 3551 Project, Optics Valley of China.

Notes

The authors declare no competing financial interest.

ACKNOWLEDGMENTS

This research was supported by the National Key Research and Development Program of China (2017YFC1104402), the Initial Research fund from China Scholarship Council and 3551 Project, Optics Valley of China. The authors are thankful for the supports.

ABBREVIATIONS

CS	chitosan
ECH−CS	epoxidized RCS
FTIR-ATR	attenuated total reflectance-Fourier transform infrared
HDA-CS	hexanediamine−chitosan
RCS	reduced chitosan
SEM	scanning electron microscopy
SHBG	sex hormone-binding globulin

REFERENCES

(1) Kaufman, J. M.; Vermeulen, A. The decline of androgen levels in elderly men and its clinical and therapeutic implications. *Endocr. Rev.* **2005**, *26* (6), 833−876.

(2) Chan, J. M.; Stampfer, M. J.; Giovannucci, E. L. What causes prostate cancer? A brief summary of the epidemiology. *Semin. Cancer Biol.* **1998**, *8* (4), 263−273.

(3) Zheng, Z.; Li, J.; Liu, Y.; Shi, Z.; Xuan, Z.; Yang, K.; Xu, C.; Bai, Y.; Fu, M.; Xiao, Q.; et al. The Crucial Role of AR-V7 in Enzalutamide-Resistance of Castration-Resistant Prostate Cancer. *Cancers* **2022**, *14* (19), 4877.

(4) Kan, W. C.; Hsieh, K. L.; Chen, Y. C.; Ho, C. H.; Hong, C. S.; Chiang, C. Y.; Wu, N. C.; Chen, M.; Shih, J. Y.; Chen, Z. C.; et al. Comparison of Surgical or Medical Castration-Related Cardiotoxicity in Patients with Prostate Cancer. *J. Urol.* **2022**, *207* (4), 841−850.

(5) Freedland, S. J.; Abrahamsson, P. A. Androgen deprivation therapy and side effects: Are GnRH antagonists safer? *Asian J. Androl.* **2021**, *23* (1), 3−10.

(6) Crawford, E. D.; Heidenreich, A.; Lawrentschuk, N.; Tombal, B.; Pompeo, A. C. L.; Mendoza-Valdes, A.; Miller, K.; Debruyne, F. M. J.; Klotz, L. Androgen-targeted therapy in men with prostate cancer: Evolving practice and future considerations. *Prostate Cancer Prostatic Dis.* **2019**, *22* (1), 24−38.

(7) Feldman, B. J.; Feldman, D. The development of androgen-independent prostate cancer. *Nat. Rev. Cancer* **2001**, *1* (1), 34−45.

(8) Dunn, J. F.; Nisula, B. C.; Rodbard, D. Transport of steroid hormones: Binding of 21 endogenous steroids to both testosterone-

binding globulin and corticosteroid-binding globulin in human plasma. *J. Clin. Endocrinol. Metab.* **1981**, *53* (1), 58−68.
(9) Vermeulen, A.; Verdonck, L. Studies on the binding of testosterone to human plasma. *Steroids* **1968**, *11* (5), 609−635.
(10) Hendriks, F. K.; Wiersma, J.; van der Sande, F. M.; Alexander, S. E.; Kooman, J. P.; Bons, J. A. P.; van Loon, L. J. C. Hemodialysis does not lower circulating testosterone concentrations. *J. Nephrol.* **2024**, *37* (4), 1125−1127.
(11) Ghannoum, M.; Bouchard, J.; Nolin, T. D.; Ouellet, G.; Roberts, D. M. Hemoperfusion for the Treatment of Poisoning: Technology, Determinants of Poison Clearance, and Application in Clinical Practice. *Semin. Dial.* **2014**, *27* (4), 350−361.
(12) Ronco, C.; Bellomo, R. Hemoperfusion: Technical aspects and state of the art. *Crit Care* **2022**, *26* (1), 135.
(13) Avvakumov, G. V.; Muller, Y. A.; Hammond, G. L. Steroid-binding specificity of human sex hormone-binding globulin is influenced by occupancy of a zinc-binding site. *J. Biol. Chem.* **2000**, *275* (34), 25920−25925.
(14) Blindauer, C. A.; Harvey, I.; Bunyan, K. E.; Stewart, A. J.; Sleep, D.; Harrison, D. J.; Berezenko, S.; Sadler, P. J. Structure, properties, and engineering of the major zinc binding site on human albumin. *J. Biol. Chem.* **2009**, *284* (34), 23116−23124.
(15) Yu, H.; Ke, H.; Chen, T.; Li, X.; Tan, S.; Zhou, L.; Wang, S. Zn 2+ -loaded cellulose beads stabilized by chitosan and prepared via freeze-drying for removing human testosterone in plasma. *Artif. Cells, Nanomed., Biotechnol.* **2018**, *46* (sup 2), 912−920.
(16) Majdoubi, H.; Şimşek, S.; Billah, R. E. K.; Koçak, N.; Kaya, Ş.; Tamraoui, Y.; Katin, K. P.; Hannache, H.; Marzouki, R. Novel Geopolymer Composite Based on Oil Shale and Chitosan for Enhanced Uranium (VI) Adsorption: Experimental and Theoretical Approaches. *J. Mol. Liq.* **2024**, *395*, 123951.
(17) Billah, R. E. K.; Şimşek, S.; Majdoubi, H.; Kaya, Ş.; Agunaou, M.; Soufiane, A.; Katin, K. P. Removal of Lead (II) from Aqueous Solution Using Epichlorohydrin Cross-Linked Shrimp Waste-Derived Chitosan Based @ Calcium Phosphates Biocomposite: Experimental Study and Computational Approach. *J. Mol. Liq.* **2023**, *389*, 122872.
(18) Wu, L.; Zhang, Z. Preparation of polyamidoamine dendrons supported on chitosan microspheres and the adsorption of bilirubin. *J. Appl. Polym. Sci.* **2013**, *130* (1), 563−571.
(19) Li, H. T.; Zhang, Y. M.; Chen, X. F.; Shi, K. Y.; Yuan, Z.; Liu, B.; Shen, B.; He, B. L. Synthesis and adsorption aspect of crosslinked PVA-based blood compatible adsorbents for LDL apheresis. *React. Funct. Polym.* **2004**, *58* (1), 53−63.
(20) Kong, X. Simultaneous determination of degree of deacetylation, degree of substitution and distribution fraction of -COONa in carboxymethyl chitosan by potentiometric titration. *Carbohyd. Polym.* **2012**, *88* (1), 336−341.
(21) Hong, W.; Zhi, Y.; Xin-Lian, T.; Bing-Lin, H. Investigations on the Adsorbents for Uremic Middle Molecular Toxins(I). *Chem. J. Chinese Univ.* **2002**, *23* (1), 75−77.
(22) Fu, G.; Yu, H.; Yuan, Z.; Liu, B.; Shen, B.; He, B. Chitosan adsorbents carrying amino acids for selective removal of low density lipoprotein. *Artif. Cells Blood Substitutes Biotechnol.* **2004**, *32* (2), 303−313.
(23) Minobe, S.; Watanabe, T.; Sato, T.; Tosa, T.; Chibata, I. Preparation of adsorbents for pyrogen adsorption. *J. Chromatogr. A* **1982**, *248* (3), 401−408.
(24) Sundberg, L.; Porath, J. Preparation of adsorbents for biospecific affinity chromatography: I. Attachment of group-containing ligands to insoluble polymers by means of bifunctional oxiranes. *J. Chromatogr. A* **1974**, *90* (1), 87−98.
(25) Bao, H.; Gao, X.; Zheng, X.; Li, Y. Preparation and Properties of Chitosan Immobilized Zinc Ion Affinity Chromatography Matrix. *J. Chin. Biotechnol.* **2012**, *32* (5), 85−90.
(26) Zhang, Y.; Li, Y. F.; Yang, L. Q.; Ma, X. J.; Wang, L. Y.; Ye, Z. F. Characterization and adsorption mechanism of Zn2+ removal by PVA/EDTA resin in polluted water. *J. Hazard. Mater.* **2010**, *178* (1−3), 1046−1054.
(27) Wang, S. Q.; Yu, Y. T.; Cui, T.; Cheng, Y. A novel amphiphilic adsorbent for the removal of low-density lipoprotein. *Biomater* **2003**, *24* (16), 2799−2802.
(28) Soltys, P. J.; Etzel, M. R. Equilibrium adsorption of LDL and gold immunoconjugates to affinity membranes containing PEG spacers. *Biomater* **2000**, *21* (1), 37−48.
(29) singh, A. T.; Kumar, P. S.; Kumar, K. S. Binding of Zn(II) ions to chitosan−PVA blend in aqueous environment: Adsorption kinetics and equilibrium studies. *Environ. Prog. Sustainable* **2015**, *34* (1), 15−22.
(30) Xiao, Y.; Zhou, X. Synthesis and properties of a novel crosslinked chitosan resin modified by L-lysine. *React. Funct. Polym.* **2008**, *68* (8), 1281−1289.
(31) Simsek, S.; Derin, Y.; Kaya, S.; Senol, Z. M.; Katin, K. P.; Ozer, A.; Tutar, A. High-Performance Material for the Effective Removal of Uranyl Ion from Solution: Computationally Supported Experimental Studies. *Langmuir* **2022**, *38*, 10098−10113.

https://doi.org/10.1021/acsomega.4c11595
ACS Omega 2025, 10, 15393−15399